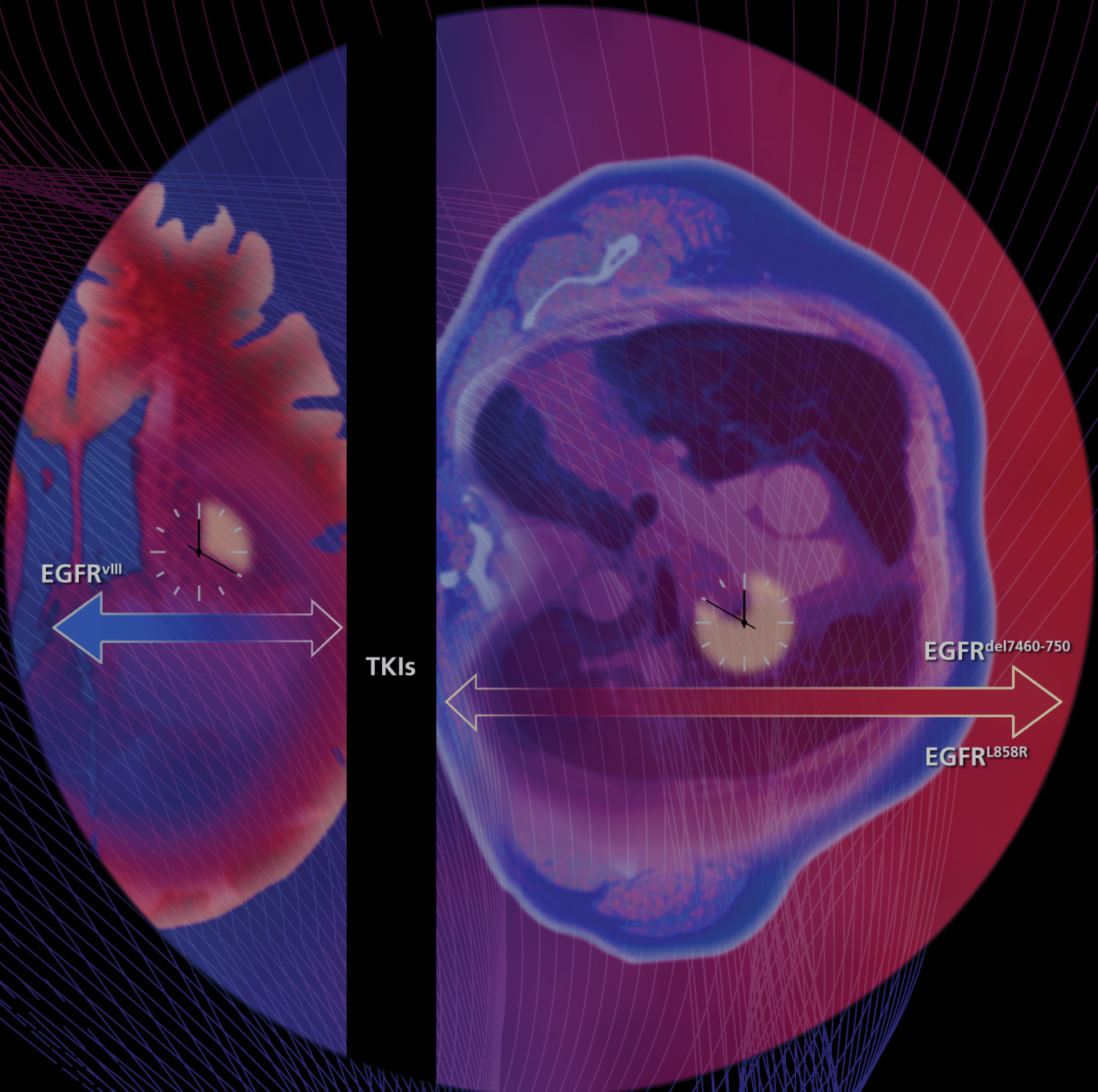


RESEARCH ARTICLE

Kinetics of Inhibitor Cycling Underlie Therapeutic Disparities between EGFR-Driven Lung and Brain Cancers

Krister J. Barkovich^{1,2}, Sujatmi Hariono², Adam L. Garske³, Jie Zhang², Jimmy A. Blair⁵, Qi-Wen Fan^{1,2}, Kevan M. Shokat^{3,4}, Theodore Nicolaides², and William A. Weiss^{1,2}



ABSTRACT

Although mutational activation of the epidermal growth factor receptor (EGFR) features prominently in glioma and non-small cell lung cancer (NSCLC), inhibitors of EGFR improve survival only in patients with NSCLC. To understand how mutations in EGFR influence response to therapy, we generated glioma cells expressing either glioma- or NSCLC-derived alleles and quantified kinase-site occupancy by clinical inhibitors with the use of a novel affinity probe and kinetic methodology. At equivalent doses, erlotinib achieved lower kinase-site occupancy in glioma-derived *EGFRvIII* compared with NSCLC-derived *EGFR* mutants. Kinase-site occupancy correlated directly with cell-cycle arrest. *EGFRvIII* released erlotinib rapidly compared with wild-type EGFR, whereas NSCLC-derived mutants released erlotinib slowly.

SIGNIFICANCE: These data suggest that kinase-site occupancy is a biomarker for efficacy of EGFR inhibitors, that rapid binding and release of erlotinib in glioma-derived *EGFRvIII* opposes the blockade of downstream signaling, and that slower cycling of erlotinib within the active site of NSCLC-derived mutants underlies their improved clinical response. *Cancer Discov*; 2(5):450–7. ©2012 AACR.

INTRODUCTION

The epidermal growth factor receptor (EGFR/HER1/ErbB1) is a transmembrane protein belonging to the EGFR family of receptor tyrosine kinases (1). EGFR is implicated as an oncogene in a large number of cancers, driving malignancy through overexpression/amplification, activating mutation, and/or decreased turnover (2). Amplification of EGFR occurs commonly in malignant glioma, the most common primary brain tumor (3). These tumors typically express a truncated form of EGFR as a result of the in-frame deletion of introns 2–7, resulting in a ligand-independent, constitutively active EGFR protein [*EGFRvIII* (4, 5)]. EGFR amplification and mutation have also been reported in non-small cell lung cancer (NSCLC), the most aggressive form of lung cancer. Ten percent of patients with NSCLC have mutations in the EGFR kinase domain, which result in activated EGFR signaling (6, 7).

Small-molecule tyrosine kinase inhibitors (TKI) of EGFR have been developed and tested clinically (8). Erlotinib (OSI-774, Tarceva; OSI Pharmaceuticals, LLC) and gefitinib (Iressa; AstraZeneca) showed poor overall responses in initial clinical trials for patients with chemotherapy-refractory NSCLC, although a subsection of patients had dramatic responses (7). In

retrospective studies in responders, investigators subsequently identified mutations within the tyrosine kinase domain of EGFR, typically point mutation in exon 21 (L858R) or in-frame deletion in exon 19 (del746–750). Biochemical analyses revealed that these mutations increased EGFR activity and led to heightened sensitivity to EGFR blockade (9).

In contrast, although in an initial study authors demonstrated an increased rate of transient radiographic responses to EGFR inhibition in malignant glioma patients with *EGFRvIII* expression (10), in subsequent trials investigators demonstrated no survival benefit (11, 12). The poor response to tyrosine kinase inhibitors (TKI) observed in patients with glioma with mutationally activated *EGFRvIII* stands in stark contrast to the dramatic response observed in NSCLC patients with activated EGFR mutations (L858R and del746–750).

Could access to brain tissue, or cell-type differences, account for this differential response to therapy? Evidence against this argument stems from observations that *EGFRvIII* is also found in approximately 5% of patients with NSCLC (13) and does not correlate with response to therapy in this group. Moreover, Ji and colleagues (13) compared human B cells transduced with lung- or brain cancer-derived alleles of EGFR (13) and demonstrated that *EGFRvIII* cells show significant resistance to TKI treatment relative to EGFR-L858R cells. These data suggest that the differential response of L858R and *EGFRvIII* is linked to the mutational status of EGFR itself.

To elucidate a mechanistic basis for the differential responses to therapy observed in lung- and brain cancer-derived alleles of EGFR, we generated isogenic cell lines containing either wild-type-, glioma-, or NSCLC-derived alleles of EGFR. Using a novel EGFR fluorescent affinity probe to measure EGFR kinase-site occupancy, we demonstrate that the differential therapeutic responses across the panel of cells correlate with differential occupancy of TKI in the kinase-active site. To provide molecular insights into these differences in occupancy, we demonstrated that brain cancer-derived alleles of EGFR released erlotinib more rapidly, whereas NSCLC-derived mutants released erlotinib more slowly in comparison with wild-type EGFR. These data provide a mechanistic basis for the differential response of lung and brain cancer

Authors' Affiliations: Departments of ¹Neurology, ²Pediatrics, Neurosurgery, Brain Tumor Research Center, Helen Diller Family Comprehensive Cancer Center, ³Cellular and Molecular Pharmacology, and ⁴Howard Hughes Medical Institute, University of California, San Francisco; and ⁵Department of Developmental Biology, Stanford University, Stanford, California

Note: Supplementary data for this article are available at Cancer Discovery Online (<http://www.cancerdiscovery.aacrjournals.org>).

Corresponding Authors: William A. Weiss, Departments of Neurology, Pediatrics, Neurosurgery, Brain Tumor Research Center, and Helen Diller Family Comprehensive Cancer Center, 1450 Third Street, HD 277, MC 0520, San Francisco, CA 94158-9001. Phone: 415-502-1694; Fax: 415-476-0133; E-mail: waweiss@gmail.com; Theodore Nicolaidis, Departments of Pediatrics, Neurosurgery, Brain Tumor Research Center, and Helen Diller Family Comprehensive Cancer Center, 533 Parnassus Ave, M649, Box 0106, San Francisco, CA 94143. Phone: 415-476-3831; Fax: 415-502-4372; E-mail: Theodore.Nicolaidis@ucsf.edu

doi: 10.1158/2159-8290.CD-11-0287

©2012 American Association for Cancer Research.

patients to EGFR TKIs and highlight kinase-site occupancy as a prominent biomarker for efficacy.

RESULTS

Erlotinib Treatment Inhibits Growth in a Mutant EGFR-Specific Manner

To control for cell type-specific effects, wild-type *EGFR*, *EGFRvIII*, *EGFR L858R*, and *EGFRdel746-750* were transduced individually into glioma cell lines U87MG and LN229MG. Because *PTEN* may also drive resistance to EGFR TKIs (14), we chose cell lines both wild-type (LN229MG) and mutant (U87MG) for *PTEN*. As expected (5, 9) the variant III, L858R, and del746-750 *EGFR*-mutants exhibited increased basal EGF-independent phosphorylation compared with the wild-type EGFR (Fig. 1A). Flow cytometric analysis demonstrated the 4 *EGFR* alleles show differential responses to erlotinib (Fig. 1B), with comparable results observed in LN229MG cells (Supplementary Fig. S1). A similar trend was also observed in cell viability in both the U87MG and LN229MG *EGFR* allele panels (Supplementary Fig. S2). These cell-based observations were thus aligned with clinical data from patients treated with erlotinib.

Quantifying Kinase-Site Occupancy in Mutant-EGFR Alleles

We previously developed a fluorescent probe specific to the active site of EGFR by attaching an NBD fluorophore via a PEG linker to the C7 position of PD168393, a 6-acrylamido-4-anilinoquinazoline that binds irreversibly to Cys797 of EGFR (15). Despite the highly conserved nature of the kinase active site, the presence of this cysteine is rare among receptor tyrosine kinases, affording this probe, affinity probe 16 (compound 16), high

specificity for EGFR (16). In our previous study we validated the capacity of this probe to measure the kinase-site occupancy of anilinoquinazoline derivatives in analog-sensitive alleles. Here, we show that affinity probe 16 also has high specificity for wild-type EGFR, as well as the glioma- and NSCLC-derived mutants (Supplementary Fig. S3).

Erlotinib Achieves Allele-Specific Differences in Kinase-Site Occupancy in Lung- and Brain Cancer-Derived Mutants of EGFR

Cells were treated with erlotinib, and then subjected to a short pulse-chase of the EGFR-fluorescent affinity probe 16, on ice. Because affinity probe 16 can only bind unoccupied active sites, this method quantifies open kinase sites across the different mutant alleles. The binding of erlotinib to EGFR is dynamic. Thus, a fraction of erlotinib-bound EGFR will become unoccupied during the affinity probe 16 pulse and will become available for compound 16 binding. Therefore, affinity probe 16 labeling quantifies the amount of kinase site that has remained occupied during the period of probe labeling, referred to as erlotinib's kinase-site occupancy. In both drug-treated U87 and LN229 panels, erlotinib achieved significantly greater levels of kinase-site occupancy in NSCLC-derived alleles of EGFR compared with *EGFRvIII* (Fig. 2, Supplementary Fig. S4).

Kinase-Site Occupancy Is a Biomarker for Efficacy

Calculated levels of kinase-site occupancy mirrored the trend of erlotinib's efficacy observed in patients. Kinase-site occupancy was also closely aligned with cell-cycle arrest achieved by erlotinib across the panels. The correlation coefficient of open kinase site and percent dividing cells was identical, 0.92, for both the U87MG and LN229MG *EGFR* allele panels

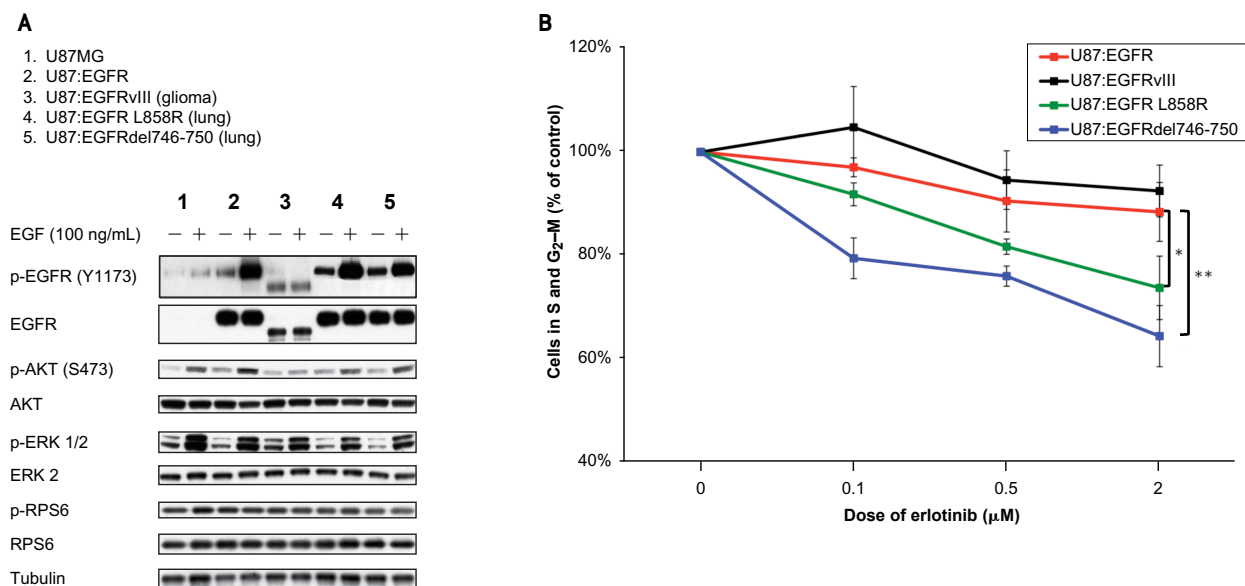
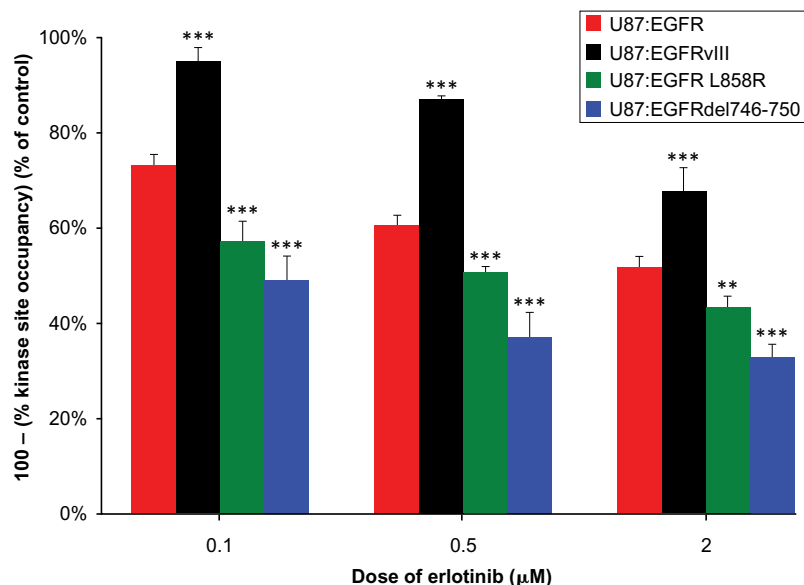


Figure 1. EGFR mutants exhibit differential growth inhibition in response to erlotinib. **A**, U87MG cells were transduced with wild-type *EGFR*, *EGFRvIII*, *EGFR L858R*, or *EGFRdel746-750*. Cells were treated or untreated with EGF 30 minutes before harvest, as shown. Cells were then lysed and analyzed by immunoblot. Signaling downstream of EGFR was analyzed with antisera to total and phospho-specific proteins shown. **B**, the U87MG panel was treated for 24 hours with 3 doses of erlotinib, as shown. Cells were analyzed for their DNA content, measured by propidium iodide staining. For each sample, the proportion of cells in S- and G₂-M-phases was combined and graphed. Treatments were completed in triplicate with error bars representing 1 SD (**P* < 0.05, ***P* < 0.01).

Figure 2. *EGFR* alleles differ in levels of kinase-site occupancy achieved after erlotinib treatment. The U87MG panel was treated overnight with erlotinib at doses shown and stimulated for 30 minutes with 100 ng/mL EGF. Cells were subjected to a 25-minute pulse-chase with 60 μ M affinity probe 16, then lysed and separated by SDS-PAGE. Gels were scanned on a Typhoon fluorescence imager with a 488-nm excitation laser. Levels of fluorescence correspond to the amount of kinase active site that is unbound by erlotinib ($100 - [\% \text{ kinase-site occupancy}]$), and thus is available for probe binding. The fluorescence intensity for each treatment was quantified by densitometry and scaled as a percentage of the EGF-stimulated control lane. Results were completed in triplicate, with error bars representing 1 SD (** $P < 0.01$, *** $P < 0.005$).



(Fig. 3A and B). These data suggest kinase-site occupancy as a biomarker for the differential efficiency of erlotinib across tumor-derived, activated alleles of *EGFR*. In addition, different mutationally activated alleles of *EGFR* all showed identical trends between kinase-site occupancy and proliferation in 2 different cell lines (Supplementary Fig. S5). Thus, data in Figure 3 and Supplementary Figure S5 demonstrate that allele-specific differences in kinase occupancy are the major arbitrator distinguishing differential sensitivity to erlotinib.

Antiproliferative Effects of Erlotinib Correlate Poorly with Abundance of Phosphorylated EGFR

Using the reversible *EGFR* inhibitor erlotinib in the panel of wild-type and mutant alleles of *EGFR*, we assessed the relationship between kinase-site occupancy and downstream signaling (Fig. 4). Immunoblot analysis of the U87MG panel revealed a marked difference between kinase-site occupancy and abundance of phosphorylated *EGFR* (p-*EGFR*) as measured at Y1173 and global phosphorylation of *EGFR* as measured by 4G10 anti-tyrosine antibody (Supplementary Fig. S6). Analysis of the Western blots by the use of fluorescently-coupled secondary antibodies and densitometry revealed coefficients of 0.71 and 0.50 for the correlation of kinase-site occupancy with p-*EGFR* (Y1173) and p-Tyr (4G10), respectively. Weak correlations were also measured between antiproliferative efficacy and abundance of p-*EGFR* (Y1173) and p-Tyr (4G10), with correlation coefficients of 0.68 and 0.52, respectively (Supplementary Figs. S7 and S8). The weak overall correlation between p-*EGFR* levels and efficacy was the result of differences in the cell-cycle response of each allele, at similar abundances of p-*EGFR* (Supplementary Fig. S9), visualized by the differences in the trend lines for each allele. These observations suggest that p-*EGFR* levels are a poor biomarker for erlotinib's efficacy across *EGFR* alleles.

The abundance of p-*EGFR* also did not accurately reflect abundance of downstream pathway targets p-AKT and p-ERK1/2. In contrast, levels of kinase-site occupancy correlated more accurately with levels of p-ERK1/2 and moderately with levels of p-AKT, although clearly this correlation was imperfect (Fig. 4). Similar results were observed in both U87MG and LN229MG *EGFR* allele panels, arguing that these effects

were both independent of *PTEN* status and not specific to a particular allele of *EGFR*. The abundance of p-AKT and p-ERK1/2 was particularly sensitive to erlotinib in NSCLC-derived mutants, as compared with glioma-derived *EGFR*vIII, shown clearly in the *PTEN*^{WT} LN229 panel (Supplementary Fig. S10). Studies in U87 and LN229 cells expressing a mutant form of *EGFR* that is resistant to erlotinib [*EGFR* T790M (17, 18)] suggest that this effect is not attributable to any off-target effects of erlotinib (Supplementary Fig. S11). This observation demonstrates that kinase-site occupancy accurately reflects oncogenic signaling through downstream molecules.

Differences in Kinetics of Erlotinib Binding and Release Underlie Differential Erlotinib Occupancy Observed in Brain Cancer- Versus Lung Cancer-Derived Mutants of EGFR

To probe the basis for differential kinase-site occupancy, we analyzed the kinetics of erlotinib binding to *EGFR*. Erlotinib-*EGFR* binding follows a simple equilibrium reaction, with *EGFR* existing in either erlotinib-bound or erlotinib-unbound states at all times. However, this reaction is difficult to probe in a cellular setting without altering either *EGFR* or erlotinib in a way that would also change their relative interactions.

Exploiting the fact that the fluorescent affinity probe 16 binds all studied *EGFR* alleles irreversibly and with a greater affinity than erlotinib, we used compound 16 to analyze the kinetics of *EGFR* binding to erlotinib across the panel of *EGFR* alleles. *EGFR* binds irreversibly to compound 16 through the covalent linkage of Cys797 to compound 16. Thus, the reaction of Cys797 with compound 16 acts as a sink for *EGFR*, preventing it from taking part in the equilibrium reaction with erlotinib. Because compound 16 has a greater affinity than erlotinib for the active site of *EGFR*, compound 16 will, over time, replace erlotinib within the active site. Therefore, the rate with which compound 16 exchanges with erlotinib can be used as a tool for studying the kinetic interaction between *EGFR* and erlotinib (detailed in the legend to Supplementary Fig. S12).

When analyzing these kinetics (Supplementary Fig. S12), we found a gradual replacement of erlotinib by compound 16 over time, represented by an increase in compound 16

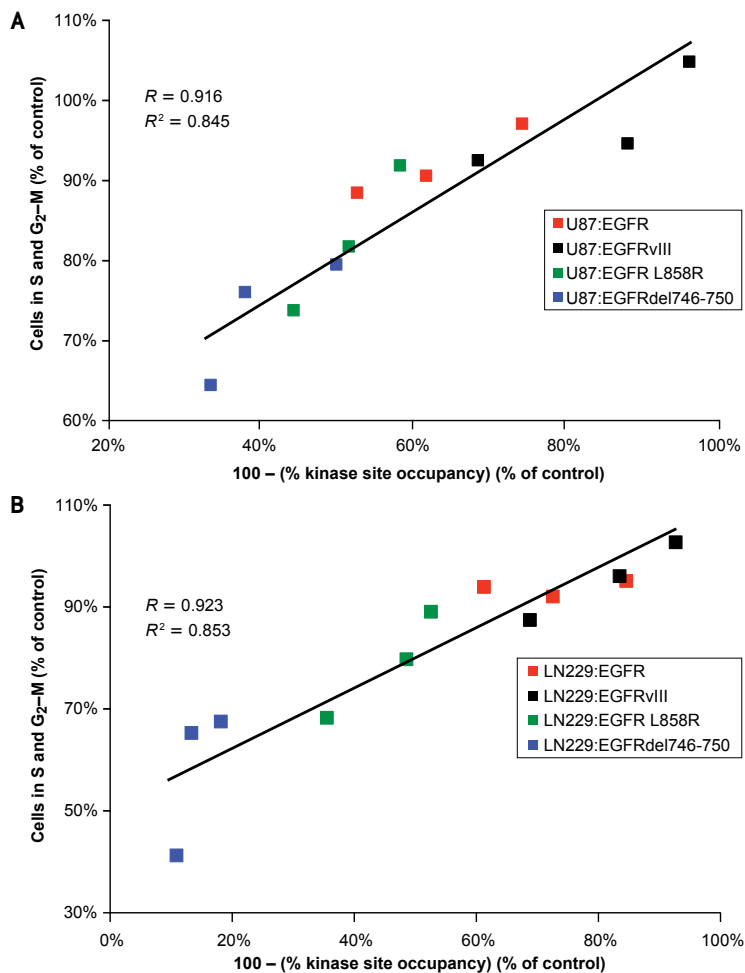


Figure 3. Kinase-site occupancy as a biomarker for efficacy of erlotinib. **A**, for each *EGFR* allele and at each dose of erlotinib, $100 - (\% \text{ kinase site occupancy})$ was assigned the x-coordinate. The proportion of cells in S- and G₂-M-phases was combined and graphed on the y-coordinate. We found a strong ($R = 0.916$) correlation between kinase-site occupancy and efficacy for the U87 panel. **B**, the same analysis was applied to the LN229 panel, where a correlation of $R = 0.923$ was found between kinase-site occupancy and efficacy.

binding to EGFR (Fig. 5A and B). Mirroring our previous experiments, the rate replacement in the glioma-derived EGFRvIII was greater than that of the wild-type allele. In contrast, NSCLC-derived EGFR L858R and EGFRdel746-750 both showed slower rates of replacement (Fig. 5C). Analysis of the clinical EGFR inhibitor, gefitinib, confirmed that these results were not erlotinib specific (Supplementary Fig. S13).

To quantify these observations, we determined the time taken for half of the EGFR within the cell to be bound by compound 16, $\tau_{1/2}$ (Table 1). The values of $\tau_{1/2}$ represent the relative time during which erlotinib occupies the active site of each *EGFR* allele, as compared with wild-type EGFR. The inverse of $\tau_{1/2}$ is also related to the speed ($V_{\text{release,Erl}}$) with which erlotinib moves in and out of the active site of each *EGFR* allele. These measurements establish the basis for the differential kinase occupancy demonstrated in Figures 2 to 4, with erlotinib cycling in and out of the active site of EGFRvIII rapidly in comparison with wild-type EGFR. In contrast, erlotinib moves in and out of the active site of NSCLC-derived alleles of EGFR much more slowly in comparison with wild-type EGFR. Analogous results were reached with the use of gefitinib (Supplementary Table S1).

DISCUSSION

Although TKIs of EGFR are now in widespread clinical use, therapeutic efficacy varies greatly among tumor types

and associated *EGFR* alleles (19). In this report, we describe a method for the determination of efficacy by measuring kinase-site occupancy, the level of total protein bound by an active site inhibitor, through the use of an active-site specific fluorescent affinity probe. Erlotinib and gefitinib, small-molecule inhibitors of EGFR, achieved greater levels of kinase-site occupancy in lung cancer-derived mutants of *EGFR* as compared with a commonly occurring glioma-derived allele. Kinase-site occupancy correlated directly with cell-cycle arrest. These data suggest kinase-site occupancy as a biomarker for efficacy.

We reported previously that in cells treated with an irreversible EGFR inhibitor, kinase-site occupancy reflected the abundance of both p-EGFR and of its downstream oncogenic signaling through AKT and ERK 1/2 (15). In this report, when the reversible clinical inhibitors erlotinib and gefitinib were used, the abundance of p-EGFR was reduced to nearly basal levels at very low doses, whereas much greater doses were required to reduce its oncogenic signaling and decrease growth. Furthermore, levels of kinase-site occupancy were aligned better with the abundance of p-AKT and p-ERK 1/2 than with abundance of p-EGFR. That this disconnect was observed upon reversible, but not irreversible, EGFR inhibition suggests that the kinetics of reversible inhibitor cycling underlie therapeutic efficacy.

In our kinetic analyses, all 3 mutant kinases differed dramatically from wild-type EGFR in the rate with which erlotinib moved in and out of the active site, quantified by the

constants $t_{1/2}$ and $V_{\text{release, Erl}}$. As a result of these differential kinetics, glioma-derived EGFRvIII required greater concentrations of erlotinib to achieve similar levels of kinase-site occupancy. Therefore, higher doses of erlotinib were required to decrease downstream signaling in glioma-derived EGFRvIII than in wild-type EGFR while lower doses were required in lung-derived EGFR L858R and EGFRdel746-750.

How do these data explain the disconnect observed between the abundance of p-EGFR and growth inhibition? We propose that at all studied doses, the half-life with which erlotinib occupies the active site of EGFR is sufficient to prevent significant ATP catalysis and autophosphorylation of tail tyrosine residues. However, the period of occupancy required to reduce oncogenic signaling of downstream molecules is longer and is only reached at doses of erlotinib or gefitinib sufficient to rapidly reoccupy the EGFR active site and maintain high levels of kinase site blockade.

Our study argues that wild-type EGFR and EGFRvIII are viable small-molecular therapeutic targets and that erlotinib fails to produce a survival advantage in malignant glioma because it fails to achieve sufficient levels of kinase-site occupancy in glioma-derived *EGFR* alleles. The use of irreversible EGFR inhibitors, and combinatorial blockade of both EGFR and of key downstream outputs, represent important areas of investigation to improve overall pathway inhibition.

METHODS

Cell Culture

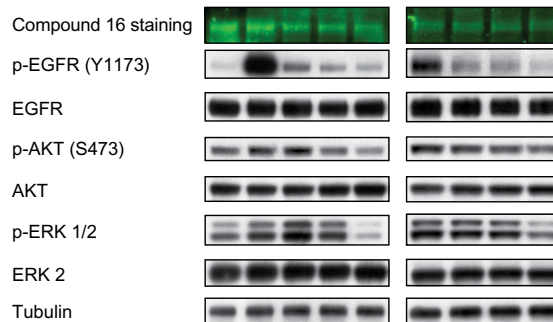
U87MG and LN229MG cell lines were obtained from American Type Culture Collection and were authenticated by the use of STR DNA fingerprinting at UCSF with use of the Promega Powerplex 1.2 platform. pcDNA3.1 plasmids containing human full-length *EGFR* or *EGFRvIII* cDNA were a gift from Dr. C. David James (UCSF), and plasmids containing *EGFR L858R* or *EGFRdel746-750* were a gift from Dr. Susumu Kobayashi (Harvard Medical School). The EGFR constructs were digested with *XhoI* and *SalI*, ligated into pWZLhygro vector, and transduced into U87MG and LN229MG cells with the use of retrovirus.

Cells were maintained in phenol red-free Dulbecco's modified Eagle medium high glucose (DME H-21) supplemented with 10% fetal bovine serum and 1% penicillin-streptomycin. Low-serum media for signaling experiments contained 1% fetal bovine serum. Cells were stored at 37°C in a 5% CO₂ incubator. For Western blot analysis, cells were plated in 6-well plates at full serum for 24 hours, and then changed to low-serum media for 24 hours before being treated in the same media for an additional 24 hours. For flow cytometric analysis, cells were plated in 6-well plates at full serum for 24 hours, and then treated in the same media for an additional 24 hours. For viability assays, cells were plated at 2×10^3 cells per well in a 24-well plate and treated once for 3 days. Media were changed before each treatment. Cell viability was determined using a WST-1 assay (Roche), according to manufacturer's instructions.

EGFR Tyrosine Kinase Inhibitors and EGFR-Specific Fluorescent Probe

Erlotinib tablets (Genentech) were purchased, ground to powder, and dissolved in aqueous HCl. The aqueous phase was extracted with ethyl acetate. The combined organic extracts were dried over sodium sulfate and concentrated to yield pure erlotinib, which was dissolved at 10 mM in dimethyl sulfoxide (DMSO) for storage at -20°C. Working dilutions of erlotinib were made immediately before use by serial dilution in low-serum media. The EGFR-specific fluorescent probe, affinity probe 16 (MW: 837g/mol), was also dissolved to 10 mM in DMSO and protected from light in storage at -20°C. The working

	U87:EGFR					U87:EGFRvIII			
Erlotinib (μM)	-	-	0.1	0.5	2	-	0.1	0.5	2
EGF (100 ng/mL)	-	+	+	+	+	-	-	-	-
100 - (% kinase site occupancy)	86	100	74	62	53	100	97	88	69



	U87:EGFR L858R					U87:EGFRdel 746-750				
Erlotinib (μM)	-	-	0.1	0.5	2	-	-	0.1	0.5	2
EGF (100 ng/mL)	-	+	+	+	+	-	+	+	+	+
100 - (% kinase site occupancy)	90	100	58	52	44	92	100	50	38	33

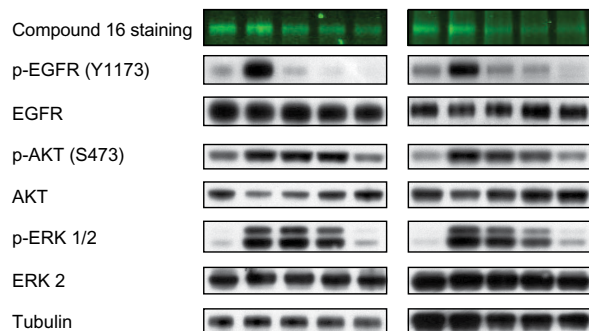


Figure 4. Antiproliferative effects of erlotinib correlate poorly with abundance of p-EGFR. The U87MG panel was treated with 3 doses of erlotinib, as shown, then pulsed with 100 ng/mL EGF before harvesting. Phospho- and total protein levels were visualized by Western blotting. Although low dosages of erlotinib efficiently blocked p-EGFR (Y1173) in all cell lines, levels of p-ERK 1/2 (T202/Y204) were decreased in NSCLC-derived alleles, compared with brain cancer-derived EGFRvIII, paralleling the antiproliferative response in Figure 1B. U87MG cells are mutant for PTEN, disconnecting signaling between EGFR and PI3K. Thus, the differential abundance of p-AKT (S473) was less apparent in this experiment, as compared with PTEN^{WT} LN229 cells (Supplementary Fig. S10). Levels of kinase-site occupancy more closely follow abundance of phosphorylated downstream molecules.

dilution was made by diluting the stock concentration 1:10 in an 85:15 PBS:DMSO mixture, and spinning at top speed in a table-top centrifuge for 10 minutes to remove the precipitate.

Western Blotting

Six-well plates were pulsed with 100 ng/mL human recombinant EGF (Roche), when applicable, for 30 minutes, then washed with ice-cold PBS. Protein was harvested from cultured cells with the use of cell lysis buffer (Cell Signaling) supplemented with complete protease inhibitor cocktail (Roche). Equal amounts of protein, as determined by a BCA Protein Assay (Thermo Scientific), were loaded into a 4% to 12% sodium dodecyl sulfate-polyacrylamide gel for electrophoresis and transferred to polyvinylidene difluoride membrane. Membranes were blocked in 5% nonfat milk dissolved in TBS-Tween 20 for 1 hour, and

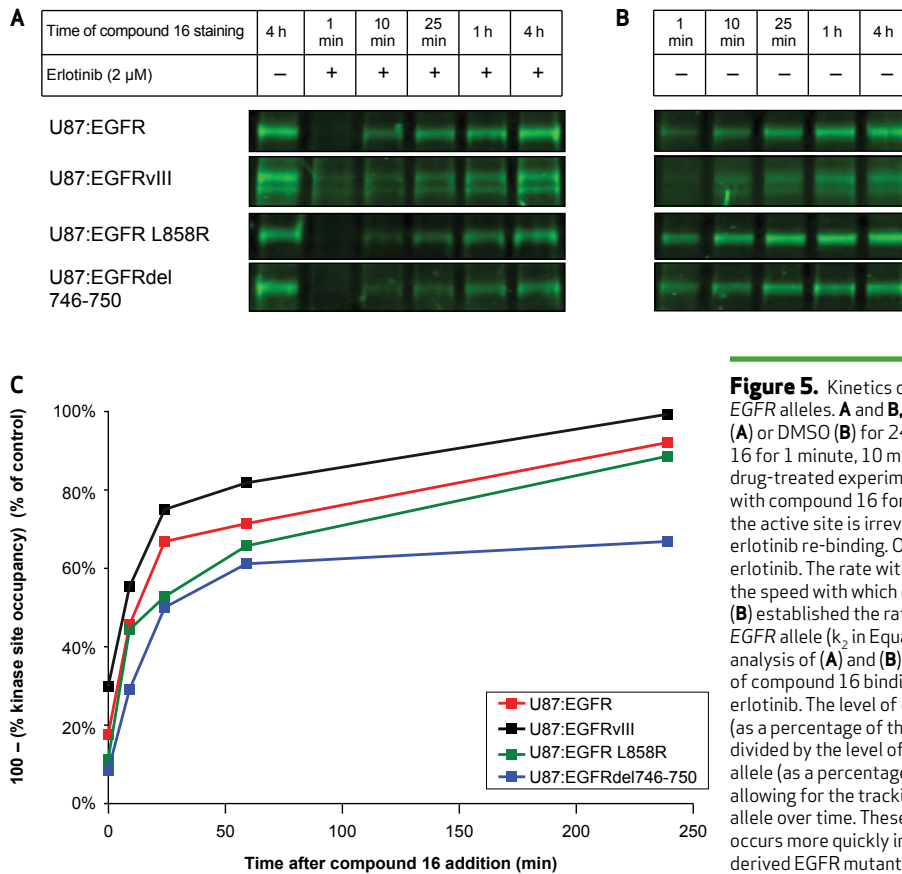


Figure 5. Kinetics of erlotinib binding/unbinding differ across *EGFR* alleles. **A** and **B**, the U87 panel was treated with 2 μ M erlotinib (**A**) or DMSO (**B**) for 24 hours and then pulsed with 60 μ M compound 16 for 1 minute, 10 minutes, 25 minutes, 1 hour, or 4 hours. In the drug-treated experiment (**A**), the control was untreated and pulsed with compound 16 for 4 hours. As erlotinib cycles out of *EGFR*, the active site is irreversibly bound by compound 16, preventing erlotinib re-binding. Over time, this occurs with all *EGFR*-bound erlotinib. The rate with which this replacement occurs is related to the speed with which erlotinib is unbound by *EGFR*. The control (**B**) established the rate at which compound 16 alone binds each *EGFR* allele (k_2 in Equation 2; see Supplementary Fig. S12 legend). **C**, analysis of (**A**) and (**B**) by densitometry allowed for the quantification of compound 16 binding over time in the presence or absence of erlotinib. The level of compound 16 staining of a single *EGFR* allele (as a percentage of the 4-hour control lane) determined in (**A**) was divided by the level of compound 16 staining of that same *EGFR* allele (as a percentage of the 4-hour control lane) determined in (**B**), allowing for the tracking of kinase-site occupancy for each *EGFR* allele over time. These data determine that erlotinib replacement occurs more quickly in glioma-derived *EGFRvIII* than in NSCLC-derived *EGFR* mutants.

then incubated overnight at 4°C in primary antibody in 5% bovine serum albumin. Mouse antiphospho-tyrosine (4G10) was obtained from Upstate Biotechnology. Rabbit anti-ERK 2, anti-*EGFR*, and anti-phospho-*EGFR* (Y1173) were obtained from Santa Cruz Biotechnology. Rabbit anti-AKT, anti-phospho-AKT (S473), anti-p44/42 MAPK, anti-rpS6, and anti-phospho-rpS6 (S235/S236) were obtained from Cell Signaling. Mouse anti- β -tubulin was obtained from Millipore. Antibodies were detected with HRP-conjugated goat antimouse or goat antirabbit secondary antibodies (Calbiochem) followed by enhanced chemiluminescence (GE Healthcare) or with DyLight 680 dye-coupled anti-rabbit secondary antibodies (Thermo Scientific) and imaged using a LI-Cor Odyssey Imaging System (LI-Cor Biosciences).

Fluorescent Gels

Six-well plates were pulsed with EGF and washed with ice-cold PBS (as described previously), then pulsed with a 60- μ M fluorescent probe for 25 minutes on ice. Cells were then harvested and run on a gel (as described previously). Gels were rinsed in a solution of 15% methanol and 5% Transfer Buffer (Invitrogen) for 20 minutes, then scanned on a Typhoon fluorescence imager (Molecular Dynamics) with the use of a 488-nm laser and a 560-nm low-pass emission filter. The fluorescent intensity was measured with the use of ImageJ software (NIH, 2008). The net band signal was determined by subtracting the fluorescent intensity of the gel below the band from the fluorescent intensity of the band. The band intensity of the control was normalized to 100%, and all subsequent band intensities scaled accordingly.

Flow Cytometry

Cells were washed with PBS then harvested with 0.25% trypsin. All media and PBS were collected for analysis. Cells were pelleted

and resuspended in PBS without Ca^{2+} and Mg^{2+} ions, permeabilized with ice-cold 70% ethanol, and then placed on ice for at least 30 minutes. Cells were then washed once with PBS then resuspended in PBS containing RNaseA (Invitrogen, 1:100) and 10 μ g/mL propidium iodide (Invitrogen). Cells were sorted with the use of FACSCalibur (Becton, Dickinson) and analyzed for their level

Table 1. Kinetic constants of *EGFR* variants panel with erlotinib

	Calculated $t_{1/2}$, min	Relative $t_{1/2}$	$V_{\text{release,Erl}}$
U87:EGFR	10.75	1.00	1.00
U87:EGFRvIII	5.89	0.55	1.83
U87:EGFR L858R	18.16	1.69	0.59
U87:EGFRdel746-750	25.30	2.35	0.43

Relative $t_{1/2}$ values for panel of *EGFR* alleles. Data from Figure 5 were fit to an equation of the form of Equation A:

$$f(t) = \frac{At}{B+Ct} + D$$

The derived function was used to calculate the $t_{1/2}$, the time after which one half of the *EGFR* active site has been bound by compound 16. The values of $t_{1/2}$ represent the relative speed with which each allele of *EGFR* releases erlotinib ($V_{\text{release,Erl}}$). The relative $t_{1/2}$ was calculated by scaling all values relative to the $t_{1/2}$ of the wild-type kinase. The inverse of this value provides the rate, relative to wild-type *EGFR*, with which the mutant *EGFR* alleles release erlotinib. $V_{\text{release,Erl}}$ and is related to erlotinib's period of occupancy of each kinase site.

of propidium iodide staining using ModFit LT 3.2 (Verity). Ten thousand live cell events were collected per treatment.

Analysis of the Kinetics of the Binding of Erlotinib to EGFR Alleles

Cells were plated as described previously for Western blotting and treated for 24 hours with 2 μ M erlotinib or 1 μ M gefitinib to allow the EGFR drug reaction to reach equilibrium. Cells were then harvested after 1 minute, 10 minutes, 25 minutes, 1 hour, or 4 hours of treatment with 60 μ M compound 16 on ice. A single control lane that was not treated with drug was treated with compound 16 for 4 hours, allowing for comparison with the nontreating compound 16-binding assay. The experiment was repeated with 24 hours of DMSO treatment as a control, which determined the differences in compound 16 binding to each EGFR allele. The level of compound 16 staining of a single drug-treated EGFR allele (as a percentage of the 4-hour control lane) was divided by the level of compound 16 staining of that same EGFR allele after DMSO treatment (as a percentage of the 4-hour control lane), allowing for the tracking of kinase site occupancy for each EGFR allele over time, corrected for differences in the kinetics of compound 16-binding for each EGFR allele.

To determine the $t_{1/2}$ of erlotinib and gefitinib replacement by compound 16, the experimental kinetic data was best fit to an equation of the form of Equation A using the solver function of Microsoft Excel to minimize the sum of the differences between the calculated value of compound 16-binding and the experimental values.

$$f(t) = \frac{At}{B+Ct} + D \quad (A)$$

Using these experimentally determined equations, we determined the $t_{1/2}$ for each EGFR allele. The relative value of $t_{1/2}$ was determined by dividing the calculated value of the $t_{1/2}$ of each EGFR allele by that of the wild type.

Statistical Analysis

For statistical comparison, a Student one-tailed *t* test was used, with *P* values of < 0.05 considered significant.

Disclosure of Potential Conflicts of Interest

No potential conflicts of interest were disclosed.

Authors' Contributions

Conception and design: K.J. Barkovich, A.L. Garske, Q.W. Fan, K.M. Shokat, T. Nicolaides, W.A. Weiss

Development of methodology: K.J. Barkovich, A.L. Garske, J.A. Blair, K.M. Shokat, T. Nicolaides

Acquisition of data: K.J. Barkovich, T. Nicolaides

Analysis and interpretation of data: K.J. Barkovich, Q.W. Fan, T. Nicolaides

Writing, review, and/or revision of the manuscript: K.J. Barkovich, T. Nicolaides, W.A. Weiss

Administrative, technical, or material support: S. Hariono, J. Zhang, T. Nicolaides

Study supervision: K.M. Shokat, T. Nicolaides, W.A. Weiss

Acknowledgments

The authors thank Trever Bivona and Neil Shah for critical review of the manuscript and Igor Vivanco, H. Ian Robins, Tim Cloughesy, and Ingo K. Mellingerhoff for sharing unpublished data.

Grant Support

This work was supported by grants from Accelerate Brain Cancer Cure, the Burroughs Wellcome Fund, the Frank A. Campini Foundation, the Howard Hughes Medical Institute, NIH K08NS065268, NIH P50CA097257, and the Samuel Waxman Cancer Research Foundation.

Received November 8, 2011; revised February 15, 2012; accepted March 13, 2012; published OnlineFirst March 31, 2012.

REFERENCES

- Holbro T, Civenni G, Hynes NE. The ErbB receptors and their role in cancer progression. *Exp Cell Res* 2003;284:99-110.
- Zandi R, Larsen AB, Andersen P, Stockhausen M-R, Poulsen HS. Mechanisms for oncogenic activation of the epidermal growth factor receptor. *Cell Signal* 2007;19:2013-23.
- Frederick L, Wang X-Y, Eley G, James CD. Diversity and frequency of epidermal growth factor receptor mutations in human glioblastomas. *Cancer Res* 2000;60:1383-7.
- Sagawa N, Ekstrand AJ, James CD, Collins VP. Identical splicing of aberrant epidermal growth factor receptor transcripts from amplified rearranged genes in human glioblastomas. *Proc Natl Acad Sci U S A* 1990;87:8602-6.
- Huang H-JS, Nagane M, Klingbeil CK, Lin H, Nishikawa R, Ji X-D, et al. The enhanced tumorigenic activity of a mutant epidermal growth factor receptor common in human cancers is mediated by threshold levels of constitutive tyrosine phosphorylation and unattenuated signaling. *J Bio Chem* 1997;272:2927-35.
- Paez JG, Jänne PA, Lee JC, Tracy S, Greulich H, Gabriel S, et al. EGFR mutations in lung cancer: correlation with clinical response to gefitinib therapy. *Science* 2004;304:1497-500.
- Lynch TJ, Bell DW, Sordella R, Gurubhagavatula S, Okimoto RA, Brannigan BW, et al. Activating mutations in the epidermal growth factor receptor underlying responsiveness of non-small-cell lung cancer to gefitinib. *N Engl J Med* 2004;350:2129-39.
- Arteaga CL. ErbB-targeted therapeutic approaches in human cancer. *Exp Cell Res* 2003;284:122-30.
- Yun C-H, Boggon TJ, Li Y, Woo MS, Greulich H, Meyerson M, et al. Structures of lung-cancer derived EGFR mutants and inhibitor complexes: mechanism of activation and insights into differential inhibitor sensitivity. *Cancer Cell* 2007;11:217-27.
- Mellinghoff IK, Wang MY, Vivanco I, Haas-Kogan DA, Zhu S, Dia EQ, et al. Molecular determinants of the response of glioblastomas to EGFR kinase inhibitors. *N Engl J Med* 2005;353:2012-24.
- Van den Bent MJ, Brandes AA, Rampling R, Kouwenhoven MCM, Kros JM, Carpentier AF, et al. Randomized phase II trial of erlotinib versus temozolomide or carmustine in recurrent glioblastoma: EORTC brain tumor group study 26034. *J Clin Oncol* 2009;27:1268-74.
- Brown PD, Krishnan S, Sarkaria JN, Wu W, Jaekle KA, Uhn JH, et al. Phase I/II trial of erlotinib and temozolomide with radiation therapy in the treatment of newly diagnosed glioblastoma multiforme: North Central Cancer Treatment Group Study N0177. *J Clin Oncol* 2008;26:5603-9.
- Ji H, Zhao X, Yuza Y, Shimamura T, Li D, Prottopopov A, et al. Epidermal growth factor receptor variant III mutations in lung tumorigenesis and sensitivity to tyrosine kinase inhibitors. *Proc Natl Acad Sci U S A* 2006;103:7817-22.
- Berger AH, Knudson AG, Pandolfi PP. A continuum model for tumor suppression. *Nature* 2011;476:163-9.
- Blair JA, Rauth D, Kung C, Yun C-H, Fan Q-W, Rode H, et al. Structure-guided development of affinity probes for tyrosine kinases using chemical genetics. *Nat Chem Biol* 2007;3:229-38.
- Singh J, Dobrusin EM, Fry DW, Haske T, Whitty A, McNamara DJ. Structure-based design of a potent, selective, and irreversible inhibitor of the catalytic domain of the erbB receptor subfamily of protein tyrosine kinases. *J Med Chem* 1997;40:1130-5.
- Kobayashi S, Boggon TJ, Dayaram T, Jänne PA, Kocher O, Meyerson M, et al. EGFR mutation and resistance of non-small-cell lung cancer to gefitinib. *N Engl J Med* 2005;352:786-92.
- Pao W, Miller VA, Politi KA, Riely GJ, Somwar R, Zakowski MF, et al. Acquired resistance of lung adenocarcinomas to gefitinib or erlotinib is associated with a second mutation in the EGFR kinase domain. *PLoS Med* 2005;2:e73.
- Ciardiello F, Tortora G. EGFR antagonists in cancer treatment. *N Engl J Med* 2008;358:1160-74.

CANCER DISCOVERY

Kinetics of Inhibitor Cycling Underlie Therapeutic Disparities between EGFR-Driven Lung and Brain Cancers

Krister J. Barkovich, Sujatmi Hariono, Adam L. Garske, et al.

Cancer Discovery 2012;2:450-457. Published OnlineFirst March 31, 2012.

Updated version	Access the most recent version of this article at: doi: 10.1158/2159-8290.CD-11-0287
Supplementary Material	Access the most recent supplemental material at: http://cancerdiscovery.aacrjournals.org/content/suppl/2012/03/15/2159-8290.CD-11-0287.DC1

Cited articles	This article cites 19 articles, 7 of which you can access for free at: http://cancerdiscovery.aacrjournals.org/content/2/5/450.full#ref-list-1
-----------------------	---

Citing articles	This article has been cited by 9 HighWire-hosted articles. Access the articles at: http://cancerdiscovery.aacrjournals.org/content/2/5/450.full#related-urls
------------------------	---

E-mail alerts	Sign up to receive free email-alerts related to this article or journal.
----------------------	--

Reprints and Subscriptions	To order reprints of this article or to subscribe to the journal, contact the AACR Publications Department at pubs@aacr.org .
-----------------------------------	--

Permissions	To request permission to re-use all or part of this article, use this link http://cancerdiscovery.aacrjournals.org/content/2/5/450 . Click on "Request Permissions" which will take you to the Copyright Clearance Center's (CCC) Rightslink site.
--------------------	--